(Article begins on next page)

Homology modelling-driven study leading to the discovery of the first mouse Trace Amine-Associated Receptor 5 (TAAR5) antagonists

Elena Cichero[a]*, Stefano Espinoza[b], Michele Tonelli[a], Silvia Franchini[c], Andrey S. Gerasimov[d], Claudia Sorbi[c], Raul R. Gainetdinov[b,d,e], Livio Brasili[c] and Paola Fossa[a]

[a]Department of Pharmacy, University of Genoa, Viale Benedetto XV,3 - 16132 Genoa, Italy

[b]Department of Neuroscience and Brain Technologies, Istituto Italiano di Tecnologia, Genova, Italy

[c]Department of Life Sciences, University of Modena and Reggio Emilia, Via Campi 183, 41125 Modena, Italy

[d]Institute of Translational Biomedicine, St. Petersburg State University, 199034, St. Petersburg, Russia

[e]Skolkovo Institute of Science and Technology, Skolkovo, 143025, Moscow Region, Russia

Corresponding author

*Elena Cichero. E-mail: cichero@unige.it, phone: +39-010-3538370

Notes

The authors declare no competing financial interest

1

Abstract

Several recent studies have focused on a detailed analysis of the trace amine-associated receptor type 5 (TAAR5) pharmacology, up to now revealing only a limited number of species-specific ligands, being also active towards other TAAR receptors. In this context, we developed our work on TAAR5 applying a structure-based computational protocol, revolving around homology modeling and virtual screening calculations. In details, *m*TAAR5 and *h*TAAR5 homology models were built, in order to explore any pattern of structural requirements which could be involved in species-specific differences. Successively, the *m*TAAR5 model was employed to perform a virtual screening of an in-house library of compounds, including different five membered ring derivatives, linked to a phenyl ring through a flexible or a rigid basic moiety. The computational protocol applied allowed to select a number of chemical scaffolds that were tested in a biological assay leading to the discovery of two first *m*TAAR5 antagonists.

Keywords: mTAAR5 antagonists, Trace amine associated receptor 5; T_1AM; molecular docking; virtual screening; homology modelling

Introduction

Trace amine-associated receptors (TAARs) belong to the family of G-protein coupled receptors (GPCR), whose first deorphanized member TAAR1 responds to a class of biogenic compounds called trace amines (TAs), such as β-phenylethylamine (β-PEA)[1]. TAs are found at low levels in multiple tissues in the periphery and brain of mammals, but their physiological functions appear still unclear[2]. In this context, the recent discovery of TAARs has provided an opportunity to explore the roles of TAs and of their receptor in physiology and disease[3,4]. In particular, TAAR1 is expressed in a variety of tissues including brain, stomach, kidney, lung and intestine, but not in the olfactory epithelium (OE). On the contrary, all the other TAAR receptor were shown to be expressed in small areas of olfactory sensory neurons (OSNs) in the OE[5].

Up to now, several efforts have been focused on the investigation of the TAAR1 pharmacology [6-10]. Indeed, accumulating evidence revealed that targeting TAAR1 could provide a novel pharmacological approach for several human disorders, such as schizophrenia, depression, attention deficit hyperactivity disorder, Parkinson's disease and metabolic diseases[11-17].

On the other hand, recent studies have also explored the biological functions of TAARs, and TAAR5 in particular, beyond olfaction[18].

In particular, low level of expression of TAAR5 was found in leukocytes[19]. Furthermore, Dinter and co-workers also reported the co-expression of TAAR1 and TAAR5 in brain regions, such as the ventromedial hypothalamus (VMH) and the amygdala[20].

A better understanding of the TAAR5 pharmacology could contribute not only to the understanding of the physiological relevance of TAAR5 but also provide an opportunity to evaluate effectiveness of new compounds selective toward this particular TAAR receptor in experimental pathological conditions.

At present, only a limited number of TAAR5 agonists are known, while no antagonist has been discovered yet. In particular, trimethylamine (**TMA**) showed both murine TAAR5 (*m*TAAR5) and human TAAR5 (*h*TAAR5) agonist activity (although only at high concentration in *h*TAAR5), while

dimethylethylamine (**DMEA**) activated only the *m*TAAR5 receptor[18].

Furthermore, 3-iodo-thyronamine (**T₁AM**) proved to display an agonist and inverse agonist profile for the *m*TAAR5 and *h*TAAR5 proteins, respectively, being also active as TAAR1 ligand[20] (Figure 1).

On this basis, the species-specificity and selectivity issues within TAAR receptors have rendered the exploration of TAAR5 pharmacology an urgent need in medicinal chemistry.

Consequently, the discovery of selective ligands is strongly required to derive suitable tools for studying TAAR5 receptor physiological role, using appropriate in vitro and/or in vivo models.

In absence of X-ray crystallographic data on this GPCR and limited number of ligands known, the rational design of TAAR5 compounds can be addressed following a proper structure-based (SB) molecular modelling protocol.

In the present study we first focused on the development of *m*TAAR5 and *h*TAAR5 homology models (HMs), in order to investigate any pattern of structural requirements which could turns in species-specific differences. In addition, we also performed a careful comparison with those HMs previously built about the *m*TAAR1 and *h*TAAR1 receptors[21,22], in order to derive new insights guiding for selectivity between the TAAR1 and TAAR5 receptors.

Furthermore, we applied a virtual screening procedure for *m*TAAR5 ligands, based on an in-house dataset of molecules previously synthesized and published as 5HT₁ₐ receptor ligands[23-29], which were already employed for *in silico* and biological screening towards TAAR1[30].

Following this computational strategy, two compounds acting as *m*TAAR5 antagonists were identified and validated in subsequent biochemical studies for the first time, representing a novel useful tool for analysis of TAAR5 physiology and pharmacology.

Thus, these data in tandem with more recent findings about TAAR5 could provide exciting new avenues for the development of innovative therapies concerning central nervous system.

Results and Discussion

*m*TAAR5 and *h*TAAR5 Homology Modeling

As shown in Figure 2**,** both *m*TAAR5 and *h*TAAR5 models were derived starting from the alignment of the two GPCR fasta sequences (Q5QD14 and O14804, respectively) on the X-ray coordinates of human β_2 adrenoreceptor (β_2-ADR; pdb code:3PDS)[31], following a procedure previously described for the TAAR1 HM[21,22]. The reliability of the alignment was verified by the high value of the pairwise percentage residue identity evaluated between *m*TAAR5 and *h*TAAR5 with respect to the human β_2 adrenoreceptor, being quite comparable (PPRI = 35.5% and 36.2%, respectively).

Accordingly, a consistent number of residues resulted to be conserved between the three GPCRs, as here reported following the specific *m*/*h*TAAR5 amino acid numbering: (*i*) L46, V49, G51, N52, V55, A58, F62, L65 residues in TM1 (helix region: 31-61), (*ii*) T67, T69, N70, S75, L76, A77, A79, D80, G84, L85, V87, P89 in TM2 (helix region: 68-96), (*iii*) F105, C107, T111, D114, L116, S121, I122, L125, C126, I128, D131, R132, A135, I136 (the β_2-adrenoreceptor DRY motif corresponded to the m/hTAAR5 DRH one, 131-133 residues) in TM3 (helix region: 104-136), (*iv*) the T147, A151, I155, W159 residues in TM4 (helix region: 148-171), (*v*) N197, F208, V210, P211, I214, M215, Y219, F223, A226, R228, Q229 in TM5 (helix region: 198-231), (*vi*) E247, H249, A250, K252, T253, L254, G255, I256, G259, G259, C264, W265, L266, P267, F268, V274 (the CWXP motif; 264-267 residues wherein m/hTAAR5 X: L266), in TM6 (helix region: 246-277), (*vii*) V286, W292, Y295, N297, S298, N301, P302, I304, Y305 (the NPXZY sequence; 301-305 residues wherein m/hTAAR5 X: I303 and Z: I304) in TM7 (helix region: 284-307).

The derived *m*TAAR5 and *h*TAAR5 models were superimposed to the coordinates of the human β_2 adrenoreceptor (Fig. 3), used as template for the homology modelling calculations, displaying a quite positive root mean square deviation value (RMSD = 0.687 Å and 0.366 Å, respectively, calculated on the carbon atom alignment).

For both the two models, the backbone conformation was inspected by Ramachandran plot,

showing the presence of one outlier, corresponding to *m/h* TAAR5 Y142, in the pre-proline psi-phi

plot (see Supplementary data S1-S2), which was reasonably far from the putative ligand recognition

site. Indeed, Y142 belong to the intracellular loop between the TM3 and TM4 domains.

In addition, quality estimates for the modelled protein side-chain was also evaluated by the rotamer

energy profile, displaying absence of outliers. Finally, a qualitative assessment of the obtained

models was also performed by evaluation of an appropriate distribution of the hydrophobic and

hydrophilic properties on the *m*TAAR5 and *h*TAAR5 surfaces. In fact, as shown in Supplementary

data S3, the receptor transmembrane domain displayed hydrophobic surface properties (depicted in

orange) while the portions extended towards the extra-cellular (EC) or the intra-cellular (IC)

environments were properly depicted in cyan (hydrophilic properties).

Taken together, these data generally validate the derived models and consequently they were

retained as a useful tool for rational design process.

*m*TAAR5 and *h*TAAR5 binding site analysis

In our previous work, we identified the putative TAAR1 binding site (BS) by taking into account

the following preliminary considerations: (*i*) several serotonergic and adrenergic ligands also act as

TAAR1 agonists, (*ii*) X-ray data about the human β_2-adrenoreceptor in complex with a number of

ligands are available, (*iii*) site-directed mutagenesis data highlighting the $5HT_{1A}$ key residues for

ligand recognition are known. Together, all these information allowed us to reasonably identify the

*m/h*TAAR1 binding site[21] comparing the derived HMs with the β2-adrenoreceptor binding site[31],

and with the previously built $5HT_{1A}$ HM key residues[26,28,29]. Therefore, we revealed *m*TAAR1

D102, which is conserved among *m/h*TAAR1, *h*β2-adrenoreceptor and h5HT$_{1A}$ protein, as a

necessary anchoring point for the agonist binding. Our studies were supported by X-ray

crystallographic data and mutagenesis experiments about ADR and $5HT_{1A}$[32], respectively,

confirming the key role played by the corresponding D113 and D116. More interestingly, our

6

results were definitively validated by the following mutagenesis studies performed by Reese et al. concerning *m*TAAR1 D102[33].

In this work, being the TAAR receptors functionally and structurally highly similar, the putative *m*/*h*TAAR5 BSs were identified comparing the derived models with the previously built *m*/*h*TAAR1 ones, whose ligand interaction cavities were described following the aforementioned strongly knowledge-based strategy. A schematic representation of the overall protocol applied for TAAR binding cavities analysis was depicted in Figure 4.

In details, the pairwise percentage residue identity (PPRI) evaluated between *m*TAAR5 and the overall *m*/*h*TAAR1 sequences proved to be of 38.5% and 37.3%, respectively. On the other hand, the *h*TAAR5 PPRI with respect to *m*/*h*TAAR1 were of 36.9% and 36.6%, respectively. Notably, the PPRI calculated around the TAAR binding sites were quite higher if compared with those evaluated for the overall proteins. Accordingly, the *m*TAAR5 BS PPRI, in comparison with the *m*/*h*TAAR1 BSs, proved to be of 44.0% and 51.7%, respectively. The one of *h*TAAR5 BS with respect to the *m*/*h*TAAR1 BSs were of 40.0% and 51.7%, respectively. Finally, the derived *m*TAAR5 and *h*TAAR5 interaction cavities resulted to be highly similar to each other, being the corresponding PPRI of 91.3% and 80.8%. A detailed comparison of the conserved *m*/*h*TAAR1 and *m*/*h*TAAR5 BS residues has been reported in **Table 1**.

Table 1. Conserved residues belonging to the *m*/*h*TAAR1 and *m*/*h*TAAR5 binding sites are listed

GPCR domain	*m*TAAR1	*h*TAAR1	*m*TAAR5	*h*TAAR5
TM2	S79	S80	S91	S91
	R82	R83	R94	R94
TM3	T99	T100	T111	T111
	D102	D103	D114	D114
TM6	W261	W264	W265	W265

	F264	F267	F268	F268
	D284	D287	D288	D288
TM7	W288	W291	W292	W292
	Y291	Y294	Y295	Y295

Therefore, on this basis it was expected that the key interactions for the *m/h*TAAR5 receptors also fell around the conserved R94 in TM2 and D114 in TM3, in tandem with a number of aromatic residues of TM6 (W265, F268) and TM7 (W292, Y295). Notably, the key role of D114 is highly supported by the mutagenesis data concerning the corresponding *m*TAAR1 D102 residue[33].

Consequently, it was hypothesized that the mandatory ligand requirements also turned in one basic core linked to a proper aromatic moiety. A much more detailed comparison of the *m/h*TAAR1 and *m/h*TAAR5 binding sites was further explored by means of docking studies on the unselective TAAR1 and TAAR5 ligand **T₁AM**, as described in the following section.

Based on this information, it is expected that any further rational drug design consideration could be much more focused and reliable. In addition, the results also allowed us to better analyse the *m/h*TAAR5 binding cavities.

*m/h*TAAR1 and *m/h*TAAR5 T₁AM species-specific differences

T₁AM is as a potent *m/h*TAAR1 agonist (*m*TAAR1 EC_{50} = 112 nM), being able to stimulate cAMP release of about 16-fold over basal for *h*TAAR1. On the other hand, **T₁AM** shows a modest agonist activity in the case of the murine TAAR5 (inducing an increase of cAMP release of about 2-fold over the basal level) and an inverse agonist profile for human TAAR5 receptor (*h*TAAR5 EC_{50} = 4.4 μM)[20].

Thus, in order to carefully explore any receptor pattern of residues probably involved in species-specific differences and selectivity, **T₁AM** was docked in the *m/h*TAAR1 and *m/h*TAAR5 HMs.

Concerning the m/hTAAR1 models, **T₁AM** docking studies suggested a common salt-bridge between the protonated nitrogen atom and the mTAAR1 D102 and the hTAAR1 D103 amino acids (Figure 5).

Notably, the compound basic moiety proved to be highly stabilized into the mTAAR1 binding site, by means of additional H-bonds with the Y287 and Y291 side-chains. At the hTAAR1 receptor, the **T₁AM** amino group was surrounded by the corresponding I290 and Y294, lacking any further H-bond interaction. On the other hand, in both the two proteins, the **T₁AM** I-phenyl ring showed cation-π contacts with the conserved mTAAR1 R82 and with the hTAAR1 R83. In addition, in the mTAAR1 model, the same ring was also engaged in π-π stacking with W288.

Finally, the phenolic hydroxyl group displayed one H-bond with the mTAAR1 R86 backbone oxygen atom, and with the hTAAR1 H87 side-chain. Therefore, a proper aromatic core linked to a basic moiety, as well as to a bulky group bearing an H-bond donor or acceptor function, could guarantee the required pattern of features to efficiently interact with both the murine and human TAAR1 receptors.

Notably, the ligand positive-charged group will be maintained around the key aspartic acid much more efficiently at the mTAAR1 receptor (by the surrounding Y287 and Y291), rather than at the hTAAR1 (displaying I290 and Y294). Thus, the potency value of any ligand bearing exclusively a basic feature is expected to strongly decreases from the murine TAAR1 receptor to the human one, giving a good explanation for the species-specificity differences observed in literature about TAAR1 ligands[34].

Concerning the m/hTAAR5 HMs, the **T₁AM** protonated nitrogen atom displayed a salt-bridge with key residue D114, while the I-phenyl core and the phenolic portion showed π–π stacking interaction with the highly conserved W265, F268, and with W292, Y295, respectively. Furthermore, the phenolic ring was stabilized by cation-π contacts with the conserved R94 side-

chain.

Notably, the *m*/*h*TAAR5 I291 and Y295 corresponded to the aforementioned *m*TAAR1 Y287 and Y291, preventing to efficiently stabilize the **T₁AM** positive-charged group. Thus, the final *m*/*h*TAAR5 **T₁AM** docking poses resulted to be slightly shifted with respect to those observed at the *m*TAAR1, orienting the basic chain toward the murine F196, F287 and the human T115 (Figure 6).

Therefore, the observed switched docking mode allowed the **T₁AM** phenolic hydroxyl group to be involved in one H-bond with the *m*/*h*TAAR5 S91. Together, these data proved to be only partially in armony with those previously discussed about the **T₁AM** behaviour at the *m*/*h*TAAR1 binding sites, supporting the higher potency trend for TAAR1 receptor over the TAAR5.

In addition, in the *m*/*h*TAAR5 HMs, the I-phenyl core displayed Van der Waals contacts with L194 and I291, corresponding to the *m*TAAR1 aromatic residues F184 and Y287, and to the *h*TAAR1 V184 and I290, respectively. On these basis, it should be noticed that the *m*/*h*TAAR5 are much more similar to the human rather than to the murine TAAR1. Thus, a rigid aromatic core could be a better choice for *m*TAAR1 ligand rather than for *h*TAAR1 or *m*/*h*TAAR5 ligands. Indeed, in these cases a much more flexible core will be able to properly occupy such a receptor crevice, interacting with L194 and I291. Moreover, the introduction of an additional basic core bearing a proper H-bond function could also allow to address a specific *m*/*h*TAAR5 profile, thanks to a possible interaction with T115. Notably, this kind of hydrophilic amino acid was replaced by a hydrophobic one at the *m*/*h*TAAR1 (I103 and I104, respectively).

Concerning the *m*TAAR5 and *h*TAAR5 similarity issue, our results allowed to disclose a highly number of conserved residues among the two GPCRs, suggesting the murine receptor as an efficient pharmacological model to gain some information to be extended to the human receptor

10

environment. Interestingly, the only differences fell around the area surrounding the **T₁AM** basic moiety, including the *m*TAAR5 F196, and the corresponding *h*TAAR5 L196. Indeed, in the *m*TAAR5 receptor, F196 contributed to reinforce the **T₁AM** binding mode, by cation-π interaction with the compound basic chain, conversely to the corresponding *h*TAAR5 L196 residue. Together, all these data revealed a key role played by an efficiently maintained salt-bridge (involving the conserved aspartic residue and the ligand basic function), whose stability inevitably decreases from the murine species to the human one. Accordingly those compounds revolving around a basic core alone (such as **TMA** or **DMEA**), strongly followed the aforementioned trend.

Virtual screening and biological assays

Virtual screening studies were performed on an in-house dataset of molecules, previously synthesized and disclosed as 5HT$_{1A}$ receptor ligands[23-29].

The selected library was obtained by combining 30 different five-membered heterocyclic scaffolds (Fragment A) with a basic moiety (Fragment B) such as aryloxyalchylamines and N1-arylpiperazines 25-30 Fragment A scaffolds were selected from a series of substituted 1,3-dioxolane, 1,3-oxathiolane, 1,3-dithiolane, spiro-dioxolane, 1,4-dioxane, tetrahydrofuran, cyclopentanone-, cyclopentanol based compounds (Figure 7).

On this set of structures, we recently applied a computationally-driven strategy which allowed us to discover five *h*TAAR1 agonist and one antagonist[30]. Interestingly, the chemical structure of the most promising molecules was characterized by a dioxolane or a cyclopentanone core linked to a flexible or a rigid basic moiety. Consequently, the final data showed that an aromatic group linked through a basic chain to a proper heterocycle core could display good electronic and steric features to interact with TAAR recognition sites.

In this work, starting from the aforementioned in-house library and also from the results on

11

*h*TAAR1 studies, a further virtual screening study focused on *m*TAAR5 was performed.

Taking into account the structure-based information here discussed, a preliminary pool of molecules was selected for biological assays. In particular, our HM-driven studies allowed to hypothesize that a proper aromatic core linked to a basic moiety bearing a H-bonding group could be useful for both the TAAR1 and TAAR5 interaction. In addition, the introduction of an additional H-bond function in proximity of the basic feature could efficiently interact with T115, addressing a specific TAAR5 profile.

Based on that, the in house dataset compounds have been docked into the putative *m*TAAR5 receptor binding site and the corresponding docking poses have been compared with the previously described **T$_1$AM** selected binding mode. Indeed, from the preliminary docking results all of them displayed at least one H-bond with D114 and also displaying π–π stacking with the conserved aromatic residues W265, F268, W292 and Y295.

Following this procedure a subset of thirty analogues including dioxolane- and tetrahydrofuran-based derivatives was retained and therefore submitted to biological assays performed on *m*TAAR5.

We measured the activity of these compounds (a total number of thirty compounds were tested) using a BRET based assay[35,36] in which HEK-293 cells were transfected with *m*TAAR5, or empty vector as control, and the cAMP EPAC BRET biosensor. We used as reference compound the standard *m*TAAR5 agonist **TMA** that also in our hand increased cAMP through TAAR5 activation (EC$_{50}$= 2.1±0.13 μM). In the initial screening phase, all the compounds were tested at 10 μM either for agonistic or antagonistic activity and then, for the ones that have been found to be active, a dose response was performed. According to the following pharmacological experiments, two molecules (compounds **1** and **2**), were characterized by *m*TAAR5 antagonist activity, showing IC$_{50}$ values of 4.8±1.1μM and 29±1.4 μM, respectively (Figure 8). Interestingly, both compounds were inactive as agonist or antagonist toward the *m*TAAR1. Indeed, these compounds have been previously investigated as TAAR1 ligands in our recent paper based on virtual screening followed by

biological assays on TAAR1, and they proved to be inactive[30].

Unfortunately, a reliable pharmacological protocol about *h*TAAR5 cannot be applied at present, because of the low potency level of the available agonist **TMA**.

Indeed, the identification of a potent *h*TAAR5 agonist still represents a crucial need for the further development of any biological assay concerning this kind of receptor.

The putative binding mode of the newly discovered antagonists **1** and **2** (Figure 9) was investigated through docking studies.

Interestingly, taking into account the *m*TAAR5 HM, the dioxolane and the tetrahydrofuran derivatives displayed a switched binding mode, that in any case revolved around the formation of the required salt-bridge with D114, through the ligand basic feature. In addition, a number of π-π stacking with W265, F287 and Y295 were also detected. As shown in Figure 10, the most promising compound **1** (the S enantiomer resulted to be the most probable) efficiently arranged the diphenyl portion around R94 and H110 also displaying cation-π contacts, while the methoxy group was engaged in one additional H-bond with T115.

Interestingly, compound **1** was *m*TAAR5 antagonist, being on the contrary inactive as TAAR1 ligand. Indeed T115 was revealed as a promising anchoring point to achieve TAAR5 selectivity, corresponding to an hydrophobic residue at the *m*TAAR1 (I103). In compound **2** (the R enantiomer resulted to be the most probable), the flexible basic moiety allowed a reversed docking mode, orienting the 2-methoxyphenyl ring and the dioxolane one in proximity of S91 and T115, respectively, displaying only a weak H-bond with T115. On these basis, related analogues could be optimized shifting the methoxy substituent onto the meta or para positions of the phenyl ring in order to achieve an H-bond with S91.

Unfortunately, due to the **TMA** poor affinity trend for the human TAAR5 receptor, the aforementioned pharmacological protocol cannot be applied for *h*TAAR5.

On the other hand, with the final aim at gaining useful information which could be employed also for the development of *h*TAAR5 ligands, both the two compounds were docked into the putative *h*TAAR5 model. The **1** and **2** docking modes were located much more in the upper zone of the human receptor cavity, if compared with those observed for the murine TAAR5 (Figure 11).

Probably, the driving force moving to this kind of behaviour deals with the role played by the *h*TAAR5 L196, with respect to that of the *m*TAAR5 F196. Indeed, the phenyl residue contributes to reinforce the binding mode in the murine model, by cation-π interaction with the ligand basic moiety. On the contrary, the leucine bulky and hydrophobic nature causes an opposite effect at the human receptor. Consequently, **1** and **2** maintained the salt-bridge with D114, lacking any H-bond with T115. On the other hand, the new docking mode allowed the methoxy group of compound **2** to interact with Y295, via H-bond. On all these basis, it is expected that the dioxolane analogue rather than the tetrahydrofuran one could be much more efficient as *h*TAAR5 ligand.

Experimental

Chemistry

In this work, we virtually screened an in-house database containing about two hundred molecules, which have been previously revealed to be active as $5HT_{1A}$ and α_1 ligands[23-29].

Following the procedure described in the virtual screening section, a few number of molecules, falling in the dioxolane and tetrahydrofuran pools, were retained and submitted to biological assays. The synthesis of selected analogues **1** and **2** was described elsewhere, as reported in the aforementioned references[23-29].

Ligand preparation

14

All the chemical entities from the in-house library plus **T₁AM**, were built, parameterized (Gasteiger-Hückel method) and energy minimized within SybylX-1.0 using Tripos force field[37]. In case of racemic mixtures, both enantiomers were drawn and considered separately for calculations.

*m*TAAR5 and *h*TAAR5 Homology Modeling

Since most of the key residues characteristic of GPCRs are conserved in TAAR5 receptor, *m*/*h*TAAR5 receptor HMs were generated, starting from the X-ray structure of human β2-adrenoreceptor (PDB code: 3PDS; resolution = 3.50 Å), in complex with an agonist compound[31]. The amino acid sequence of *m*TAAR5 (Q5QD14) and *h*TAAR5 (O14804) were retrieved from the SWISSPROT database[38] while the three-dimensional structure co-ordinates file of the GPCR template was obtained from the Protein Data Bank[39].

The amino acid sequences of *m*/*h*TAAR5 TM helices were aligned with the corresponding residues of 3PDS, on the basis of the Blosum62 matrix (MOE software)[40]. The connecting loops were constructed by the loop search method implemented in MOE. The MOE output files included a series of ten receptor models which were independently built on the basis of a Boltzmann-weighted randomized procedure[41], combined with specialized logic for the handling of sequence insertions and deletions[42]. Among the derived models, there were no significant main chain deviations. The model with the best packing quality function was selected for full energy minimization. The retained structure was minimized with MOE using the AMBER94 force field[43]. The energy minimization was carried out by the 1000 steps of steepest descent followed by conjugate gradient minimization until the rms gradient of the potential energy was less than 0.1 kcal mol-1 Å-1.

The assessment of the final obtained model was performed using Ramachandran plots, generated within MOE and by the evaluation of an appropriate distribution of the hydrophobic and hydrophilic properties on the protein surface (Connolly surface, calculated with MOE).

In order to explore the energetic profile of the whole selected *m*/*h*TAAR5 models, the contact energy values of the two proteins were compared with those calculated on the X-ray structure of the

β_2 adrenoreceptor. The effective atomic contact energies (ACE) are calculated for heavy atoms of standard amino acids within a contact range of 6 Å assigning energy terms (in kcal/mol) for each contact pair, as described by Zhang and co-workers[44]. These energies were summed up for each residue in the system. In general, a high negative value indicates that the residue is predominantly in contact with hydrophobic atoms and hence to be expected in a buried protein environment. Residues with positive energy terms indicated contacts with predominantly hydrophilic atoms and were expected in more solvent exposed areas of the protein.

In addition, quality estimates for the modelled protein side-chain was also evaluated by the rotamer energy profile, displaying absence of outliers. The rotamer strain energy was calculated on the basis of the backbone-dependent rotamer library published by Dunbrack and Cohen[45]. The rotamer statistics were collected for each φ-ψ combination in 10 degree increments and smoothed with Bayesian methods. The backbone dependency of side-chain rotamers was restricted to the χ1-angle; the remaining χ angles are independent of the backbone φ-ψ values. For a given backbone φ-ψ combination, the resulting probabilities provide estimates of weakly or strongly populated side-chain rotamers in the Protein Data Bank.

T$_1$AM molecular docking studies

Starting from the putative *h*TAAR1 binding site we previously identified[21,22], relying on the high sequence similarity within the TAAR receptor family, also the most probable *m*/*h*TAAR5 binding cavities were disclosed. Therefore, **T$_1$AM** was docked in the corresponding murine and human TAAR1 and TAAR5 HMs, by means of the Surflex docking module implemented in Sybyl-X1.0[37]. Then, the best docking geometry (selected on the basis of the SurFlex scoring functions) were refined by ligand-receptor complex energy minimization (CHARMM27), by means of the MOE software.

To better refine the obtained TAAR/ligand complexes, a rotamer exploration of all side chains involved in the compound-binding was carried out. The rotamer exploration methodology was also

included in the MOE suite.

Virtual screening studies

Docking studies focused on virtual screening were also performed using the Surflex docking module of Sybyl-X1.0. On the basis of the homology modelling-driven results, the in house dataset compounds were chosen comparing the related docking poses with those obtained for **T₁AM**, taken by us as reference compound, inside *m/h*TAAR5.

In particular, those compounds displaying at least one H-bond with D114 and also π−π stacking with the conserved aromatic residues W265, F268, W292 and Y295 were taken into account for biological assays.

All calculations were carried out on a standard personal computer running under Windows XP.

Biochemistry

Bioluminescence Resonance Energy Transfer Measurement of *m*TAAR5-dependent cAMP accumulation

HEK-293 cells were transiently transfected with *m*TAAR5 or *m*TAAR1 and a cAMP BRET biosensor and then plated in a 96-well plate as described[35,36]. For time course experiments, the plate was read immediately after the addition of the agonist and for approximately 30 minutes. For the evaluation of antagonistic activity the compound of interest was added 5 minutes before the addition of the control agonist for TAAR5 that is **TMA**. All the compounds were screened with an initial concentration of 10 μM and then for the ones that were active, a dose response was performed using concentrations from 10 nM to 100 μM in order to calculate EC_{50} values. For putative antagonist, IC_{50} was calculated by measuring the effect of the compounds against the effect of 3-methylamine at 10 μM. Readings were collected using a Tecan Infinite instrument that allows the sequential integration of the signals detected in the 465 to 505nm and 515 to 555 nm windows using filters with the appropriate band pass and by using iControl software. The acceptor/donor

ratio was calculated as previously described[46]. Curve was fitted using a non linear regression and one site specific binding with GraphPad Prism 5. Data are representative of 3 independent experiments and are expressed as means±SEM.

Conclusions

In this work, a computationally-driven strategy was applied, in order to develop a careful analysis of pharmacological properties of *m/h*TAAR5 receptors. On the basis of the obtained data, the conserved residue D114 was recognized as a mandatory anchoring point for ligand interaction. In addition, thanks to a comparison with the previously built *m/h*TAAR1 HMs, species-specific and selectivity issues were also addressed. In particular, a key role played by aromatic residues around the conserved aspartic acid was shown as a critical point in efficiently stabilizing the ligand basic feature into TAAR binding site. Accordingly, the potency value of those compounds bearing exclusively a basic moiety (such as **TMA** and **DMEA**) strongly decreases from the murine TAAR receptor to the human one. As regards selectivity, our data highlighted the *m/h*TAAR5 T115 as a key residue to address a specific TAAR5 profile. All these information was supported by the virtual screening study, which definitively validate the computational strategy applied.

Notably, the screening results guided the discovery of the first selective *m*TAAR5 antagonists, compounds **1** and **2**, being one of them endowed with a good selectivity profile (TAAR5/TAAR1 > 20), opening also the possibility of future development of *h*TAAR5 ligands.

Supporting information

Ramachandran plots derived for murine and human TAAR5 homology models and graphic representation of the hydrophobic and hydrophilic surface properties.

Acknowledgments

References

[1] D.K. Grandy, *Pharmacol Ther.* 2007, **116**, 355-390.

[2] M.D. Berry, *J. Neurochem.* 2004, **90**, 257–271.

[3] B. Borowsky, N. Adham, K.A. Jones, R. Raddatz, R. Artymyshyn, K.L. Ogozalek, M.M. Durkin, P.P Lakhlani, J.A. Bonini, S. Pathirana, N. Boyle, X. Pu, E. Kouranova, E.; Lichtblau, H.; F.Y. Ochoa, T.A. Branchek, C. Gerald *Proc Natl Acad Sci U S A.* 2001, **98**, 8966–8971.

[4] J.R. Bunzow, M.S. Sonders, S. Arttamangkul, L.M. Harrison, G. Zhang, D.I. Quigley, T. Darland, K.L. Suchland, S. Pasumamula, J.L. Kennedy, S.B. Olson, R.E. Magenis, S.G. Amara, D.K. Grandy *Mol Pharmacol.* 2001, **60**, 1181–1188.

[5] S.D. Liberles, L.B. Buck *Nature* 2006, **442**, 645–650.

[6] L. Lindemann, M.C. Hoener *Trends Pharmacol Sci.* 2005, **26**: 274–281.

[7] L.S. Barak, A. Salahpour, X. Zhang, B. Masri, T.D. Sotnikova, A.J. Ramsey, J.D. Violin, R.J. Lefkowitz, M.G. Caron, R.R. Gainetdinov *Mol. Pharmacol.* 2008, **74**, 585–594.

[8] V.M. Lam, S. Espinoza, A.S. Gerasimov, R.R. Gainetdinov, A. Salahpour *Eur J Pharmacol.* 2015 pii: S0014-2999(15)30090-X. doi: 10.1016/j.ejphar.2015.06.026.

[9] S. Espinoza, G. Lignani, L. Caffino, S. Maggi, I. Sukhanov, D. Leo, L. Mus, M. Emanuele, G. Ronzitti, A. Harmeier, L. Medrihan, T.D. Sotnikova, E. Chieregatti, M.C. Hoener, F. Benfenati, V. Tucci, F. Fumagalli, R.R. Gainetdinov *Neuropsychopharmacology.* 2015, **40**, 2217-2227.

[10] S. Espinoza, V. Ghisi, M. Emanuele, D. Leo, I. Sukhanov, T.D. Sotnikova, E. Chieregatti, R.R. Gainetdinov *Neuropharmacology.* 2015, **93**, 308-313.

[11] R. Zucchi, G. Chiellini, T.S. Scanlan, D.K. Grandy *Br J Pharmacol.* 2006, **149**, 967–978.

[12] Z. Xie, S.V. Westmoreland, M.E. Bahn, G.L. Chen, H. Yang, E.J. Vallender, W.D. Yao, B.K. Madras, G.M. Miller *J Pharmacol Exp Ther.* 2007, **321**, 116–127.

[13]   Z. Xie, S.V. Westmoreland, G.M. Miller *J Pharmacol Exp Ther.* 2008, **325**, 629–640.

[14]   S. Espinoza, A. Salahpour, B. Masri, T.D. Sotnikova, M. Messa, L.S. Barak, M.G. Caron, R.R. Gainetdinov *Mol Pharmacol.* 2011, **80**, 416–425.

[15]   L. Lindemann, C.A. Meyer, K. Jeanneau, A. Bradaia, L. Ozmen, H. Bluethmann, B. Bettler, J.G. Wettstein, E. Borroni, J.L. Moreau, M.C. Hoener *J. Pharmacol. Exp. Ther*. 2008, **324**, 948–956.

[16]   T.D. Sotnikova, M.G. Caron, R.R. Gainetdinov *Mol. Pharmacol.* 2009, **76**, 229–235

[17]   D.T. Sotnikova, I.Z. Olesya, V. Ghisi, M.G. Caron, R.R. Gainetdinov *Parkinsonism Relat. Disord.* 2008, **14**, S99–S102.

[18]   I. Wallrabenstein, J. Kuklan, L. Weber, S. Zborala, M. Werner, J. Altmuller, C. Becker, A. Schmidt, H. Hatt, T. Hummel, G. Gisselmann *PloS One*, 2013, **8**, e54950. doi: 10.1371/journal.pone.0054950

[19]   D.A. Nelson, M.D. Tolbert, S.J. Singh, K.L. Bost *J Neuroimmunol.* 2007, **192**, 21-30.

[20]   J. Dinter, J. Mühlhaus, C.L. Wienchol, C.X. Yi, D. Nürnberg, S. Morin, A. Grüters, J. Köhrle, T. Schöneberg, M. Tschöp, H. Krude, G. Kleinau, H. Biebermann *PLoS One*. 2015, 10, e0117774. doi: 10.1371/journal.pone.0117774. eCollection 2015

[21]   E. Cichero, S. Espinoza, R.R. Gainetdinov, L. Brasili, P. Fossa *Chem. Biol. Drug Des.* 2013, **81**, 509-516.

[22]   G. Chiellini, G. Nesi, M. Digiacomo, R. Malvasi, S. Espinoza, M. Sabatini, S. Frascarelli, A. Laurino, E. Cichero, M. Macchia, R.R. Gainetdinov, P. Fossa, L. Raimondi, R. Zucchi, S. Rapposelli *J. Med. Chem.* 2015, **58**, 5096-5107.

[23]   L. Brasili, C. Sorbi, S. Franchini, M. Manicardi, A. Angeli, G. Marucci, A. Leonardi, E. Poggesi *J. Med. Chem.* 2003, **46**, 1504-1511.

[24]   C. Sorbi, S. Franchini, A. Tait, A. Prandi, R. Gallesi, P. Angeli, G. Marucci, L. Pirona, E. Poggesi, L. Brasili *ChemMedChem* 2009, **4**, 393-399.

[25]   S. Franchini, A. Tait, A. Prandi, C. Sorbi, R. Gallesi, M. Buccioni, G. Marucci, C. De

Stefani, A. Cilia, L. Brasili *ChemMedChem* 2009, **4**, 196-203.

[26]   S. Franchini, A. Prandi, A. Baraldi, C. Sorbi, A. Tait, M. Buccioni, G. Marucci, A. Cilia, L. Pirona, P. Fossa, E. Cichero, L. Brasili *Eur. J. Med. Chem.* 2010, **45**, 3740-3751.

[27]   S. Franchini, A. Prandi, C. Sorbi, A. Tait, A. Baraldi, P. Angeli, M. Buccioni, A. Cilia, E. Poggesi, P. Fossa, L. Brasili *Bioorg. Med. Chem. Lett.* 2010, **20**, 2017-2020.

[28]   A. Prandi, S. Franchini, L.I. Manasieva. P. Fossa, E. Cichero, G. Marucci, M. Buccioni, A. Cilia, L. Pirona, L. Brasili *J. Med. Chem.* 2012, **55**, 23-36.

[29]   S. Franchini, U.M. Battisti, A. Baraldi, A. Prandi, P. Fossa, E. Cichero, A. Tait, C. Sorbi, G. Marucci, A. Cilia, L. Pirona, L. Brasili *Eur. J. Med. Chem.* 2014, **87**, 248-266.

[30]   E. Cichero, S. Espinoza, S. Franchini, S. Guariento, L. Brasili, R.R. Gainetdinov, P. Fossa *Chem. Biol. Drug Des.* 2014, **84**, 712-720.

[31]   D.M. Rosenbaum, C. Zhang, J.A. Lyons, R. Holl, D. Aragao, D.H. Arlow, S.G.F. Rasmussen, H.J. Choi, B.T. Devree, R.K. Sunahara, P.S. Chae, S.H. Gellman, R.O. Dror, D.E. Shaw, W.I. Weis, M. Caffrey, P. Gmeiner, B.K. Kobilka *Nature* 2011, **469**, 236-240.

[32]   M. Nowak, M. Kolaczkowski, M. Pawlowski, A.J. Bojarski *J. Med. Chem.* 2006, **4**, 205–214.

[33]   E.A. Reese, Y. Norimatsu, M.S. Grandy, K.L. Suchland, J.R. Bunzow, D.K. Grandy *J. Med. Chem.* 2014, **57**, 378-390.

[34]   D.B. Wainscott, S.P. Little, T. Yin, Y. Tu, V.P. Rocco, J.X. He, D.L. Nelson *J. Pharmacol. Exp. Ther.* 2007, **320**, 475-485.

[35]   A. Salahpour, B. Masri *Nat. Methods* 2007, **4**, 599–600.

[36]   S. Espinoza, B. Masri, A. Salahpour, R.R. Gainetdinov *Methods Mol. Biol.* 2013, **964**, 107-122.

[37]   Sybyl X 1.0 Tripos Inc, 1699 South Hanley Road, St Louis, Missouri 63144, USA 25

[38]   A. Bairoch, R. Apweiler *Nucleic. Acids Res.* 2000, **28**, 45-48.

[39]   H.M. Berman, J. Westbrook, Z. Feng, G. Gilliland, T.N. Beth, H. Weissig, I.N. Shindyalov, P.E. Bourne *Nucleic Acids Res*. 2000, **28**, 235-242.

[40]   MOE: Chemical Computing Group Inc. Montreal. H3A2R7 Canada. http://www.chemcomp.comp

[41]   M. Levitt *J. Mol. Biol.* 1992, **226**, 507–533.

[42]   T. Fechteler, U. Dengler, D. Schomberg *J. Mol. Biol.* 1995, **253**, 114–131.

[43]   W.D.C.P. Cornell, C.I. Bayly, I.R. Gould, K.M. Merz, D.M. Ferguson, D.C. Spellmeyer, T. Fox, J.W. Caldwell, P.A.J. Kollman *J. Am. Chem. Soc*. 1995, **117**, 5179–5196.

[44]   C. Zhang, G. Vasmatizis, J.L. Cornette, C. DeLisi *J. Mol. Biol.* 1997, 267, 707–726.

[45]   R.L. Dunbrack, F.E. Bayesian *Protein Sci.* 1997, **6**, 1661–1681.

[46]   A. Salahpour, S. Espinoza, B. Masri, V. Lam, L. S. Barak, R.R. Gainetdinov *Front. Endocrinol.* 2012, *3*, 105. doi: 10.3389/fendo.2012.00105. eCollection 2012

Figures

Homology modelling-driven study leading to the discovery of the first mouse Trace Amine-Associated Receptor 5 (TAAR5) antagonists

Elena Cichero[a]*, Stefano Espinoza[b], Michele Tonelli[a], Silvia Franchini[c], Andrey S. Gerasimov[d], Claudia Sorbi[c], Raul R. Gainetdinov[b,d,e], Livio Brasili[c] and Paola Fossa[a]

[a]Department of Pharmacy, University of Genoa, Viale Benedetto XV,3 - 16132 Genoa, Italy

[b]Department of Neuroscience and Brain Technologies, Istituto Italiano di Tecnologia, Genova, Italy

[c]Department of Life Sciences, University of Modena and Reggio Emilia, Via Campi 183, 41125 Modena, Italy

[d]Institute of Translational Biomedicine, St. Petersburg State University, 199034, St. Petersburg, Russia

[e]Skolkovo Institute of Science and Technology, Skolkovo, 143025, Moscow Region, Russia

Corresponding author

*Elena Cichero. E-mail: cichero@unige.it, phone: +39-010-3538370

**Notes**

The authors declare no competing financial interest

**Figure 1.** Chemical structure of **T₁AM**, a TAAR1 and TAAR5 ligand.

Figure 2. Alignment of the *m*TAAR5 and *h*TAAR5 sequences on the corresponding *h*β$_2$-adrenoreceptor (*h*β$_2$-ADR) residues. The α-helix and loop domains are highlighted in red and blue. respectively.

3
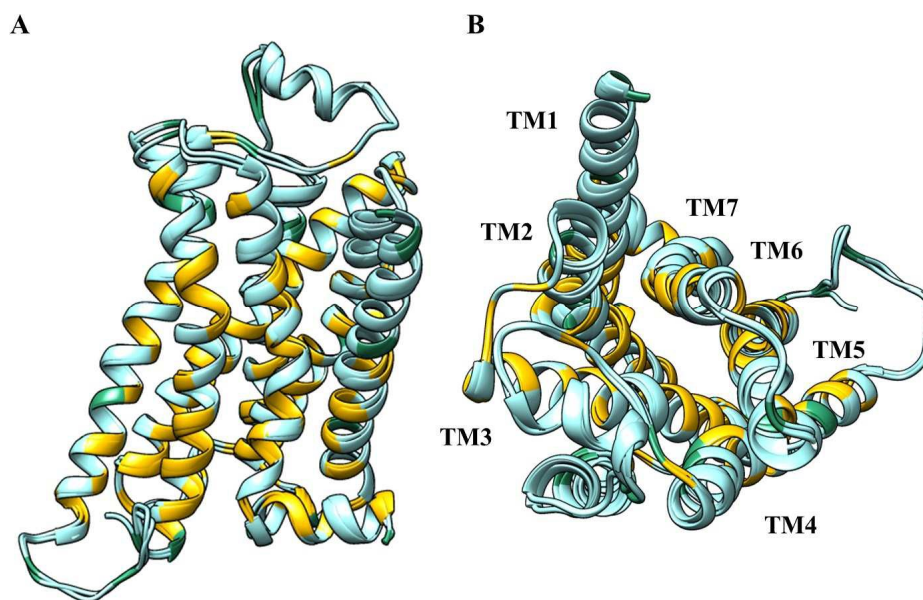
Figure 3. The superimposition of the derived *m*TAAR5 and *h*TAAR5 models on the 3PDS co-ordinates is depicted as side-view (A) and as top-view (B). The conserved regions are highlighted in yellow.
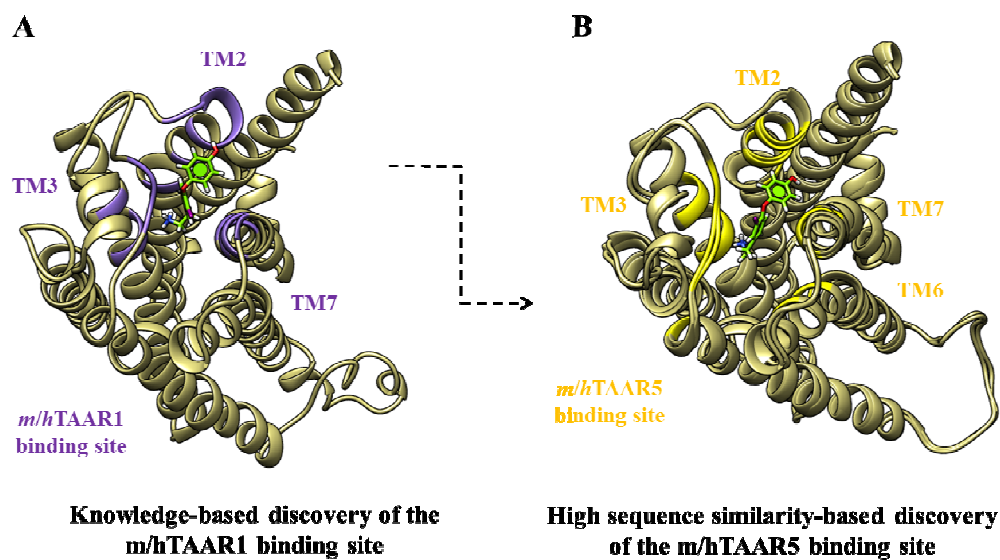
Figure 4. A schematic representation of the applied computational protocol, starting from the previously knowledge-based discovery of the *m/h*TAAR1 binding sites. The TAAR1 models guided the following identification of the highly structurally related TAAR5 BSs.

5
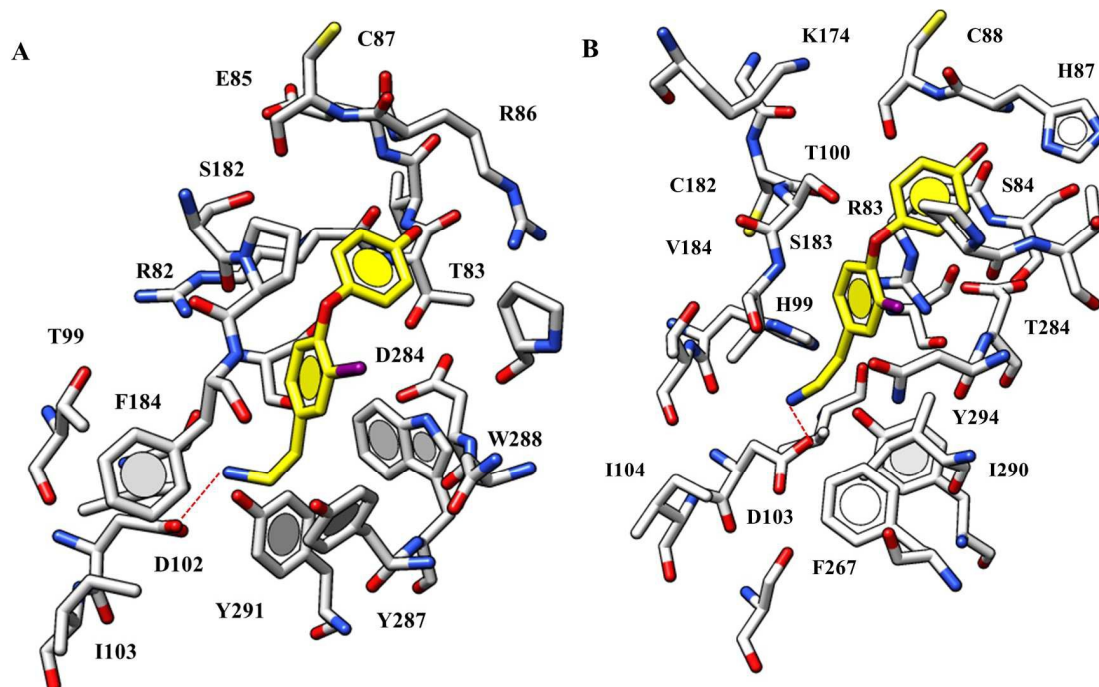
Figure 5. T₁AM docking pose into the *m*TAAR1 (A) and *h*TAAR1 (B) models. For simplicity, only the salt-bridge is depicted in red. The compound is reported in stick (C atom: yellow)
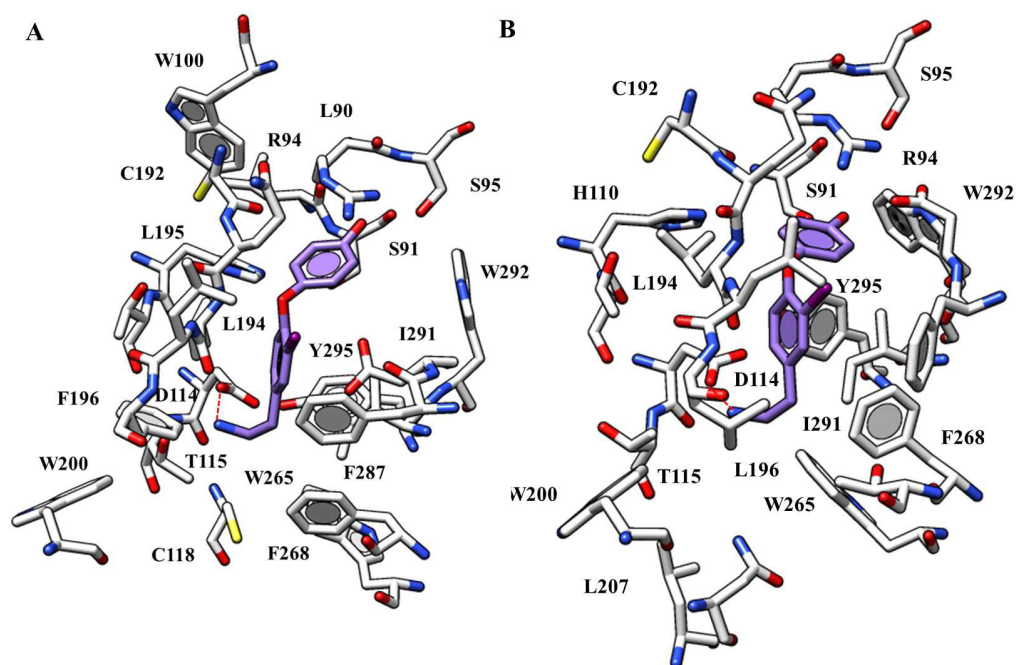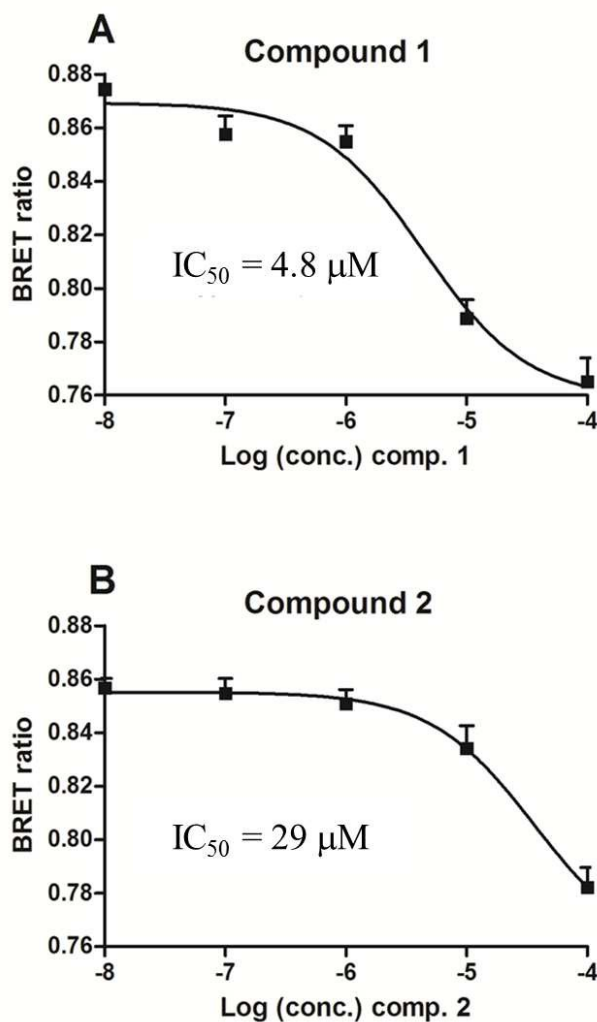
Figure 6. T₁AM docking mode into *m*TAAR5 (A) and *h*TAAR5 (B) models. For simplicity, only the salt-bridge is depicted in red. The compound is reported in stick (C atom: light purple). Only the most important residues are labelled.
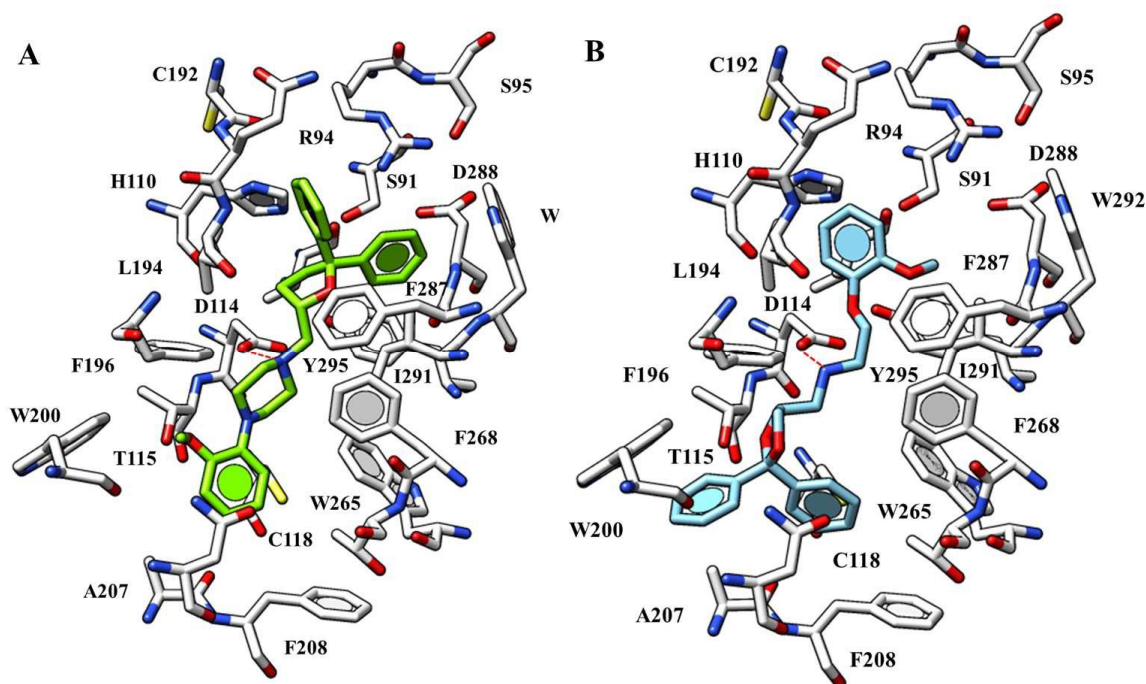
7

Figure 7. Schematic representation of the in-house dataset compounds collection.

Figure 8. cAMP variations induced by the tested compounds in cells co-expressing mTAAR5 and EPAC. Cells were treated with the compounds at different concentrations and plotted as a dose–response experiment. A non-linear regression with one site-specific binding is used to draw the curve using GraphPad Prism5. Data are plotted as means $\pm$ SEM of 3 independent experiments.

mTAAR1 IC$_{50}$ > 100 μM mTAAR1 IC$_{50}$ > 100 μM

mTAAR5 IC$_{50}$ = 4.8 μM mTAAR5 IC$_{50}$ = 29 μM
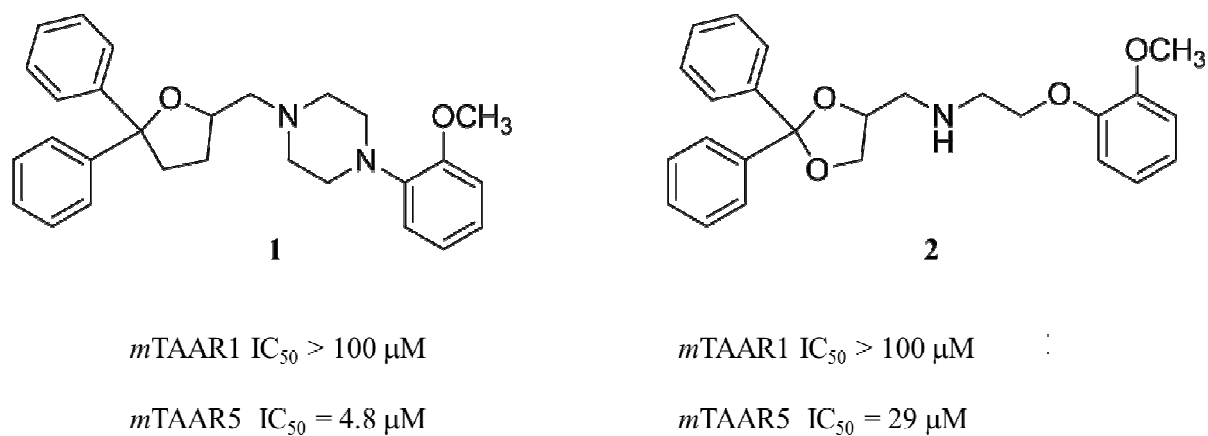
Figure 9. Chemical structure of the newly identified mTAAR5 antagonists.

10

Figure 10. Compound **1** (A) and **2** (B) docking poses into the *m*TAAR5 model. For simplicity, only the salt-bridge is depicted in red. Ligands are reported in stick (C atom: light green and cyan, respectively). Only the most important residues are labelled.

11
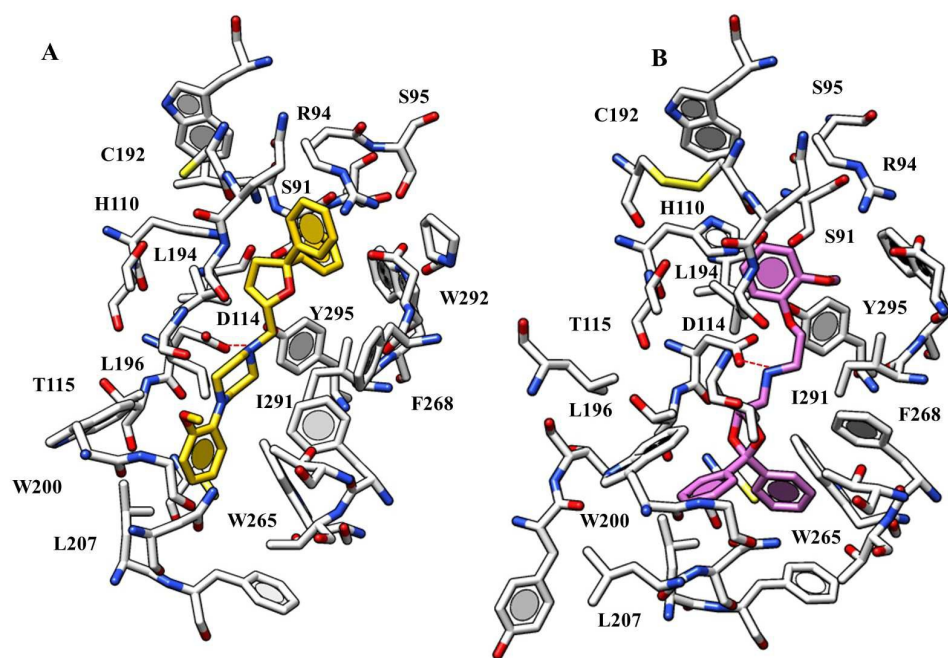
Figure 11. Compound **1** (A) and **2** (B) docking poses into the *h*TAAR5 model. For simplicity, only the salt-bridge is depicted in red. Ligands are reported in stick (C atom: gold and orchid, respectively). Only the most important residues are labelled.

12

Graphical abstract

Homology modelling-driven study leading to the discovery of the first mouse Trace Amine-Associated Receptor 5 (TAAR5) antagonists

Elena Cichero[a]*, Stefano Espinoza[b], Michele Tonelli[a], Silvia Franchini[c], Andrey S. Gerasimov[d], Claudia Sorbi[c], Raul R. Gainetdinov[b,d,e], Livio Brasili[c] and Paola Fossa[a]

[a]Department of Pharmacy, University of Genoa, Viale Benedetto XV,3 - 16132 Genoa, Italy

[b]Department of Neuroscience and Brain Technologies, Istituto Italiano di Tecnologia, Genova, Italy

[c]Department of Life Sciences, University of Modena and Reggio Emilia, Via Campi 183, 41125 Modena, Italy

[d]Institute of Translational Biomedicine, St. Petersburg State University, 199034, St. Petersburg, Russia

[e]Skolkovo Institute of Science and Technology, Skolkovo, 143025, Moscow Region, Russia

1